Hindawi Publishing Corporation
Journal of Applied Mathematics
Volume 2014, Article ID 714079, 9 pages
http://dx.doi.org/10.1155/2014/714079

Research Article

Dynamic Surface and Active Disturbance Rejection Control for Path Following of an Underactuated UUV

Juan Li, Haitao Gao, Jiajia Zhou, and Zheping Yan

College of Automation, Harbin Engineering University, Harbin 150001, China

Correspondence should be addressed to Jiajia Zhou; zhoujiajia@hrbeu.edu.cn

Received 20 December 2013; Accepted 6 February 2014; Published 19 March 2014

Academic Editor: Weichao Sun

This paper addresses the problem of accurate path following control for an underactuated unmanned underwater vehicle (UUV) in the horizontal plane. For an underactuated UUV, the line-of-sight (LOS) guidance method is adopted to map 2D reference trajectory into a desired orientation, and through the tracking of heading to achieve path following, where the sideslip is introduced to modify the desired orientation. In this paper, we propose a method called dynamic surface and active disturbance rejection control (DS-ADRC) to solve the path following control problem. This controller can effectively avoid the phenomenon of explosion of terms in the conventional backstepping method, reduce the dependence on the UUV controller mathematical model, and enhance the antijamming ability. Simulation is carried out to verify the effectiveness of the proposed control method for an underactuated UUV. The results show that, even for this controller with disturbance, the cross-track error of UUV is gradually converged to zero and has some certain robustness.

1. Introduction

The high accuracy path following mission is a typical behavior of UUVs, and it is an important method for UUVs to complete other tasks (such as topography examination and long distance navigation) [1]. Under the influences of some uncertain disturbance such as the ocean current, the UUV's movements are very complicated with six degrees of freedom (DOF).

At present, the research on UUV's tracking control mainly focuses on the following three aspects: way-point tracking [2–4], path following [5], and trajectory tracking [6]. For the path following, many scholars at home and abroad have further studies and proposed some mature control technologies in those fields of unmanned aerial vehicle (UAV), unmanned boat, the surface ship, the autonomous underwater vehicle (AUV), and so on. The path following of UUVs is usually simplified as the horizontal and vertical planes, and the controllers are designed, respectively. This paper mainly studies the problem of horizontal path following. Lapierre and Soetanto [7] designed an AUV tracking controller based on the Lyapunov method and the backstepping technique, and the AUV tracking error is gradually converged to zero. But it did not take the disturbance of the marine environment into account. Shi et al. [8] used the same method as Lapierre and Soetanto [7] and ensured the tracking error in the global asymptotic stability under the influence of the constant current. But there is a phenomenon called "explosion of terms" which may exist when we use the backstepping technique to obtain the repeated derivative of virtual control variation. Swaroop et al. [9] proposed a dynamic surface control (DSC) strategy for a class of nonlinear systems, which let the virtual control pass through a low-pass filter, where a new value was obtained to calculate the approximate derivation. This technique can avoid the phenomenon of "explosion of terms." However, even a simple dynamic surface controller design requires the accurate mathematical model of controlled object. Li et al. [10] used the active disturbance rejection control (ADRC) technology to design a path following controller for an underactuated surface ship. It could deal with the problem of the transverse drift of the ship caused by the constant wind disturbance, but the path following responds slowly with the use of a linear PD control rate.

Usually, the accurate mathematical model of an UUV is difficult to obtain. Even with a precise mathematical model, it is also so complex that it needs to do some simplification

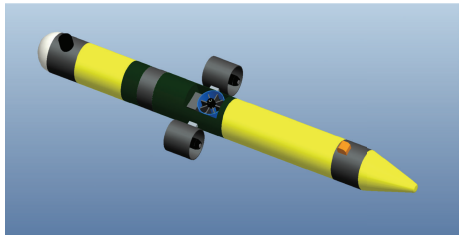

Figure 1: Minesniper MkII.

when doing control system design, which eventually leads to model error. Based on the DS-ADRC technique, this paper designs a horizontal path following controller for an underactuated UUV, which effectively avoids the "explosion of terms" phenomenon when using backstepping method and also reduces the high requirements of the dynamic surface control technology to the accurate mathematical model. It does real-time estimation to the internal and external disturbance in the loop and eventually compensates the estimation into the control system, which improves the control accuracy and has high stability.

2. Mathematical Models for MKII

This paper selects Minesniper MkII as a simulation object, which is shown in Figure 1 and based on [11]. The length of the UUV is 1.929 m and weight is 40 Kg. There are propellers equipped, respectively, on the left and right sides of the UUV, whose maximum speed is 2000 rpm, providing maximum thrust between ±80 N. Through the left and right speed difference, it achieves the steering movement. Between the two longitudinal propellers, there is a vertical propeller, whose maximum speed is 100 rpm providing a maximum thrust for ±20 N.

Here, we assume that the position vector of the UUV is $[x, y, \psi]^T$, velocity vector of the UUV is $[u, v, r]^T$ and the ocean current speed is $[u_c, v_c, 0]^T$, the UUV's relative speed is $[u_r, v_r, r]^T$,and the controlling force and moment are $[\tau_u, 0, \tau_r]^T$, and, by means of simplifying the 6-DOF model of the UUV, we get its horizontal mathematical model with ocean current as follows:

$$\begin{aligned}
\dot{u}_r &= \frac{(-d_{11}u_r + \tau_u)}{m_{11}},\\
\dot{v}_r &= \frac{(Am_{66} - Bm_{26})}{(m_{22}m_{66} - m_{26}^2)},\\
\dot{r} &= \frac{(Bm_{22} - Am_{26})}{(m_{22}m_{66} - m_{26}^2)},\\
\dot{x} &= u\cos(\psi) - v\sin(\psi),\\
\dot{y} &= u\sin(\psi) + v\cos(\psi),\\
\dot{\psi} &= r,
\end{aligned} \tag{1}$$

Table 1: UUV relevant parameters.

$m = 40$	$N_{\dot{v}} = 2.2$	$N_v = 36$
$X_{\dot{u}} = -1.42$	$X_{u_r} = 0.1$	$X_{\lvert u_r\rvert u_r} = 8.2$
$Y_{\dot{v}} = -38.4$	$Y_{v_r} = 10$	$Y_{\lvert v_r\rvert v_r} = 200$
$Y_{\dot{r}} = -2.5$	$Y_r = 5$	$I_z = 8.0$
$N_{\dot{r}} = -8.9$	$N_r = 5$	$N_{\lvert r\rvert r} = 15$

where $A = -d_{22}v_r + (d_{26} - u_r c_{26} - mu_c)r$, $B = (d_{62} - u_r c_{62})v_r - d_{66}r + \tau_r$, and

$$\begin{aligned}
m_{11} &= m - X_{\dot{u}}, \qquad d_{11} = X_{u_r} + X_{\lvert u_r\rvert u_r}\lvert u_r\rvert,\\
m_{22} &= m - Y_{\dot{v}}, \qquad d_{22} = Y_{v_r} + Y_{\lvert v_r\rvert v_r}\lvert v_r\rvert,\\
m_{26} &= -Y_{\dot{r}}, \qquad d_{26} = Y_r,\\
m_{66} &= I_z - N_{\dot{r}}, \qquad d_{62} = N_{v_r},\\
c_{26} &= m - X_{\dot{u}}, \qquad d_{66} = N_r + N_{\lvert r\rvert r}\lvert r\rvert,\\
c_{62} &= X_{\dot{u}} - Y_{\dot{v}}.
\end{aligned} \tag{2}$$

According to [11, 12], the relevant parameters and hydrodynamic coefficients in the above equations are shown in Table 1.

3. The Line-of-Sight Guidance System

Considering the underactuated UUV in this paper, we select the LOS guidance as adopted in [11–13], which converts the two-dimensional desired location to the expected heading angle. And through tracking the expected heading angle, it achieves the path following control of the vehicle.

For the horizontal path following, it can divide the expecting path into a series of points: p_k and $k = 0, 1, \ldots, n$, where $p_k = (x_k, y_k) \in R^2$. Taking the connected two points p_{k-1}, p_k on the expecting path and taking the p_{k-1} as original points to establish north-east coordination system, these have been shown in Figure 2. β_i is the included angle of the directed line segment $p_{k-1}p_k$ and the north coordinate axis, (x_t, y_t) is the real-time location coordinates of the UUV, $\psi(t)$ is the real-time heading angle of the UUV, $d(t)$ is the distance between location and the endpoint of the path, Δ is the selecting foresight vector quantity (Δ generally is selected 2–6 times long of the UUV [14]), and $\varepsilon(t)$ is the lateral error of path tracking made by the LOS guidance system. $\delta(t)$ is the included angle of current location to path endpoint ligature and the path of the UUV, $p_{\text{los}}(x_{\text{los}}, y_{\text{los}})$ is the current foresight point, ψ_d is the expecting angle, $\alpha(t)$ is the included angle of foresight vector quantity and the expected path, and R_{accept} is the switching condition of the two expected straight line segments.

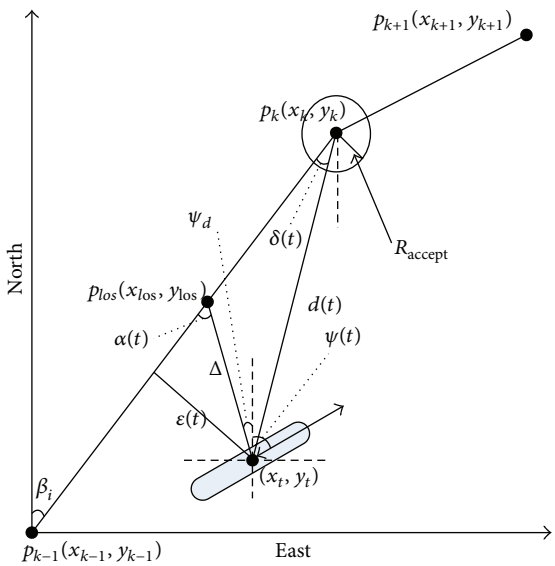

Figure 2: Line-of-sight-guidance.

Through the geometric relation, we can obtain

$$\begin{aligned}
\beta_i &= a\tan 2\left(y_k - y_{k-1}, x_k - x_{k-1}\right),\\
\delta(t) &= \beta_i - a\tan 2\left(y_k - y_t, x_k - x_t\right),\\
d(t) &= \sqrt{\left(x_k - x_t\right)^2 + \left(y_k - y_t\right)^2},\\
\varepsilon(t) &= d(t) * \sin\left(\delta(t)\right),\\
\psi_d &= \beta_i - \alpha(t).
\end{aligned} \tag{3}$$

For the selection of $\alpha(t)$, there are some certain rules. When the current position of the UUV is far away from the desired path, that is, $\varepsilon(t) > \Delta$, there are no interaction points between foresight vector and path at this time; thus there is $|\alpha(t)| = \pi/2$. When the current position of the UUV is near to the desired path, we can select $\alpha(t) = a\sin(\varepsilon(t)/\Delta)$. So we can obtain formula (4) as follows:

$$\alpha(t) = \begin{cases} a\sin\left(\dfrac{\varepsilon(t)}{\Delta}\right), & |\varepsilon(t)| \le \Delta,\\ \dfrac{\pi}{2} * \operatorname{sign}\left(\varepsilon(t)\right), & \text{others.}\end{cases} \tag{4}$$

There are currents in the case of interference; if we get the desired heading angle as desired input for the UUV control system with the above method, eventually the heading tracking is achieved, but there will be a stable track error. In this paper, in order to eliminate it, we introduce a sideslip angle $\beta = a\tan(v/u)$, the specific expression, as follows:

$$\psi_d = \beta_i - \alpha(t) - \beta. \tag{5}$$

When $d(t) < R_{\text{accept}}$ (R_{accept} is the allowable maximum error), it can select straightway $p_k p_{k+1}$ as desired path.

4. Controller Design

The horizontal movement of the UUV can be divided into two subaspects as follows [15]: one aspect is the geometrical problem, that is, controlling the position of the UUV to the expecting path, and the other one is the dynamics aspect, that is, controlling the UUV's longitudinal velocity to an expecting one. As for the former, by using the LOS guidance system, it maps the expected position instructions to the expected heading angle instructions; thus we can achieve the UUV's path following. For the latter, it is mainly to control the longitudinal propellers.

The dynamic surface control (DSC) technique has efficiently avoided the "explosion of terms" phenomenon which is caused by repeatedly instructing on the virtual controlling, but it needs the precise model of the controlled object. The active disturbance rejection control (ADRC) technique does not depend on the precise model of the controlled object, but the feedback efficiency is not high enough, and its control signal may easily have high frequency oscillation. With the help of DSC and ADRC, this paper designs a longitudinal velocity controller and a heading controller, respectively, by using the DS-ADRC method.

4.1. Model Transformation. In order to use the ADRC technique more conveniently, it firstly converts the UUV mathematical model to a standard form according to the ADRC, and then the controllers are designed, respectively.

4.1.1. Model for Heading Control. From the model of (1), it can obtain the UUV heading control mathematical model as follows:

$$\begin{aligned}
\dot{\psi} &= r,\\
\dot{r} &= \frac{\left(Bm_{22} - Am_{26}\right)}{\left(m_{22}m_{66} - m_{26}^2\right)}.
\end{aligned} \tag{6}$$

In the above model, ψ is heading angle, r is turning heading angular velocity, $A = -d_{22}v_r + (d_{26} - u_r c_{26} - mu_c)r$, $B = (d_{62} - u_r c_{62})v_r - d_{66}r + \tau_r$, $m_{22} = m - Y_{\dot{v}}$, $m_{26} = -Y_{\dot{r}}$, and $m_{66} = I_z - N_{\dot{r}}$; the specific parameters are all given in Table 1.

Assume $x_{11} = \psi$, $x_{12} = r$, and $u_1 = \tau_r$, so that we can simplify the above system as to the standard ADRC form as follows:

$$\begin{aligned}
\dot{x}_{11} &= x_{12},\\
\dot{x}_{12} &= f_1(\cdot) + b_{10}u_1,\\
y_1 &= x_{11}.
\end{aligned} \tag{7}$$

Hereinto, u_1, y_1 are the system input and output, that is, turning heading torque and heading angle, respectively, $f_1(\cdot)$ is the system nonlinear part, and b_{10} is the input gain coefficient.

Taking $u_{10} = f_1(\cdot) + b_{10}u_1$, so the above system can be converted into

$$\begin{aligned} \dot{x}_{11} &= x_{12}, \\ \dot{x}_{12} &= u_{10}, \\ y_1 &= x_{11}. \end{aligned} \tag{8}$$

4.1.2. Model for the Longitudinal Velocity Control. In the same way, from (1), we can obtain the longitudinal velocity controlling mathematical model as follows:

$$\dot{u}_r = \frac{\left(-d_{11}u_r + \tau_u\right)}{m_{11}}. \tag{9}$$

Here u_r is the UUV's relative velocity, τ_u is the longitudinal thrust, and d_{11} and $m_{11} = m - X_{\dot{u}}$ are the hydrodynamic coefficients. And the specific numerical values have been given in Table 1.

Supposing that $x_{21} = u_r$, so the above longitudinal velocity control model can be converted into the standard ADRC form as follows:

$$\begin{aligned} \dot{x}_{21} &= f_2(\cdot) + b_{20}u_2, \\ y_2 &= x_{21}. \end{aligned} \tag{10}$$

Hereinto, u_2, y_2 are the system input and output, that is, the UUV's longitudinal thrust and the longitudinal relative velocity, respectively, $f_2(\cdot)$ is the nonlinear part, and $b_{20} = 1/m_{11}$, $f_2(\cdot) = -d_{11}u/m_{11}$. The specific parameters are shown in Table 1.

Taking $u_{20} = f_2(\cdot) + b_{20}u_2$, so the above system can be converted into

$$\begin{aligned} \dot{x}_{21} &= u_{20}, \\ y_2 &= x_{21}. \end{aligned} \tag{11}$$

4.2. DSC-ADRC Controller. The ADRC controller is made up of four parts [16], including arranging transition process, extended state observer (ESO) design, nonlinear feedback law design, and dynamic compensation (DC). Compared with ADRC, the DS-ADRC controller replaces the nonlinear feedback law design in ADRC with DSC; thus the specific design process is stated as follows.

Step 1. Arrange the transition process of expected signal using the tracking-differentiator (TD). And calculate the signal v_1 and its differential v_2 from the expected signal.

Step 2. Estimate the system total disturbance through the ESO in real time.

Step 3. Calculate the part of control input u_0 based on DS-ADRC.

Step 4. Compensate the estimation using ESO to u_0. Then we can obtain the actual control input u for the UUV.

The schematic of the controller is shown in Figure 3.

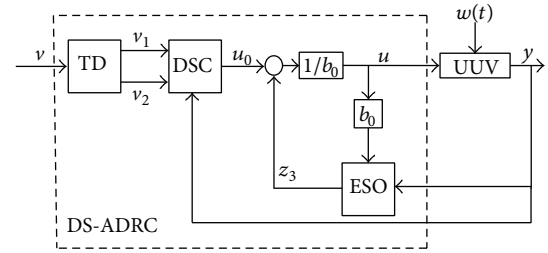

Figure 3: Design of the DS-ADRC controller.

4.2.1. Heading Controller Design

(1) TD Design. Based on the expected heading v_ψ, we arrange the transition process v_{11} and calculate its differential signal v_{12} at the same time. Thus its discrete model is written as follows:

$$\begin{aligned} fh &= fhan\left(v_{11}(k) - v_\psi(k), v_{12}(k), r, h\right), \\ v_{11}(k+1) &= v_{11}(k) + h \cdot v_{12}(k), \\ v_{12}(k+1) &= v_{12}(k) + h \cdot fh, \end{aligned} \tag{12}$$

where r is the regulation factor, h is the simulation step size, *and* $fhan(x_1, x_2, r, h)$ is the time-optimal feedback function whose specific algorithm is described as follows:

$$\begin{aligned} d &= rh, \\ d_0 &= hd, \\ y &= x_1 + hx_2, \\ a_0 &= \sqrt{d^2 + 8r|y|}, \\ a &= \begin{cases} x_2 + \dfrac{(a_0 - d)}{2}\operatorname{sign}(y), & |y| > d_0, \\ x_2 + \dfrac{y}{h}, & |y| \le d_0, \end{cases} \\ fhan &= \begin{cases} -r\operatorname{sign}(a), & |a| > d, \\ -r\dfrac{a}{d}, & |a| \le d. \end{cases} \end{aligned} \tag{13}$$

(2) ESO Design. The function of the ESO makes use of the vehicle's input and output to estimate the system's related states, including the total disturbance which acts on the system. For the heading control, the system input is the turning heading moment and its output is the heading angle; that is, $u_1 = \tau_r$ and $y_1 = \psi$, respectively. z_{11}, z_{12}, and z_{13} are the estimated values by the observer, which are induced by the heading angle, turning heading angular velocity, and

the system total disturbance, respectively. And its discrete algorithm is written as

$$\begin{aligned} e(k) &= z_{11}(k) - y_1(k), \\ fe &= fal(e(k), 0.5, \delta), \\ fe_1 &= fal(e(k), 0.25, \delta), \\ z_{11}(k+1) &= z_{11}(k) + h\left(z_{12}(k) - \beta_{11} e(k)\right), \\ z_{12}(k+1) &= z_{12}(k) + h\left(z_{13}(k) - \beta_{12} fe + b_{10} u_1(k)\right), \\ z_{13}(k+1) &= z_{13}(k) + h\left(-\beta_{13} fe_1\right), \end{aligned} \tag{14}$$

where β_{11}, β_{12}, and β_{13} are the parameters which need to be designed and $fal(e, \alpha, \delta)$ is a continuous exponential function with linear segment near the original point, whose specific algorithm is stated as follows:

$$fal(e, \alpha, \delta) = \begin{cases} \dfrac{e}{\delta^{1-\alpha}}, & |e| \le \delta, \\ |e|^{\alpha} \operatorname{sign}(e), & |e| > \delta. \end{cases} \tag{15}$$

Hereinto, δ is the length of the linear segment.

For the stability analysis of ESO, please refer to [16].

(3) DSC Design. From the converted heading control model (8), it is shown that the state of the UUV is x_{1i} and the expected state is v_{1i} calculated by TD.

Define the first dynamic surface as s_{11} as follows:

$$s_{11} = x_{11} - v_{11}. \tag{16}$$

Its first derivative is

$$\dot{s}_{11} = x_{12} - v_{12}. \tag{17}$$

Consider x_{12} as a virtual control and design a virtual stabilization function $\overline{\alpha}_{11}$:

$$\overline{\alpha}_{11} = v_{12} - k_{11} s_{11}. \tag{18}$$

where k_{11} is a positive parameter. Based on the dynamic state design method, a first-order low-pass filter can be introduced as follows:

$$\tau_{11} \dot{\alpha}_{11} + \alpha_{11} = \overline{\alpha}_{11}, \quad \alpha_{11}(0) = \overline{\alpha}_{11}(0), \tag{19}$$

where τ_{11} is the time constant of filter.

Define the second dynamic surface as s_{12}:

$$s_{12} = x_{12} - \alpha_{11}. \tag{20}$$

Its first derivative is

$$\dot{s}_{12} = \dot{x}_{12} - \dot{\alpha}_{11}. \tag{21}$$

In order to stabilize the system, we choose a variable x_{12} which satisfies

$$\dot{x}_{12} = \dot{\alpha}_{11} - k_{12} s_{12}. \tag{22}$$

Then (23) can be obtained as follows:

$$u_{10} = \dot{\alpha}_{11} - k_{12} s_{12}. \tag{23}$$

k_{12} is also a positive parameter.

The stabilization analysis of the DSC algorithm is discussed as follows. Defining $y = \alpha_{11} - \overline{\alpha}_{11}$, then there is $y = -\tau_{11} \dot{\alpha}_{11}$. Combining (17)–(22) we obtain (24) and (25), as follows:

$$\dot{s}_{11} = s_{12} + y - k_{11} s_{11}, \tag{24}$$

$$\dot{s}_{12} = -k_{12} s_{12}. \tag{25}$$

Then (26) can be obtained as follows:

$$\dot{y} = -\frac{y}{\tau_{11}} + k_{11} \dot{s}_{11} - \dot{v}_{12}. \tag{26}$$

Herein, we define $V_{1s} = s_{11}^2/2$, $V_{2s} = s_{12}^2/2$, and $V_y = y^2/2$. The derivative of V_{1s} can be calculated as

$$\begin{aligned} \dot{V}_{1s} &= s_{11}\left(s_{12} + y - k_{11} s_{11}\right), \\ \dot{V}_{2s} &= -k_{12} s_{12}^2, \\ \dot{V}_y &= -\frac{y^2}{\tau_{11}} + k_{11} y \dot{s}_{11} - y \dot{v}_{12}. \end{aligned} \tag{27}$$

Define a Lyapunov function as follows:

$$V = V_{1s} + V_{2s} + V_y. \tag{28}$$

Based on the assumption, v_{11}, v_{12}, and $\dot{v}_{12}$ are all continuous variables. Now assuming

$$\begin{aligned} s_{11}^2 + y^2 + s_{12}^2 &\le 2p, \quad \forall p < 0, \\ k_{11} \dot{s}_{11} - \dot{v}_{12} &\le q, \\ k_{1i} &= 2 + a, \quad i = 1, 2, \\ \tau_{11} &= 1 + \left(\frac{q^2}{2\varepsilon}\right) + a, \end{aligned} \tag{29}$$

then

$$\begin{aligned} \dot{V} &\le -(2+a)\left(s_{11}^2 + s_{12}^2\right) \\ &\quad + \left[\frac{\left(2s_{11}^2 + s_{12}^2 + y^2\right)}{2} + \left(1 + \frac{q^2}{2\varepsilon} + a\right) y^2 \right. \\ &\quad \left. + \frac{q^2 y^2}{2\varepsilon}\right] + \frac{\varepsilon}{2} \\ &\le -2aV + \frac{\varepsilon}{2}. \end{aligned} \tag{30}$$

When $V = p$, which satisfies $a > \varepsilon/2p$, it can be concluded that $\dot{V} < 0$.

Through the above analysis, we can know that the DSC algorithm can guarantee all the states of the closed-loop

system final convergence. And with appropriate coefficients k_{1i} and τ_{1i}, it can get a good controlling quality.

(4) DC Design. Using the estimated value z_{13} to compensate u_{10}, which obtained from the DSC. In this way, the final control variable obtained as follows:

$$u_1 = u_{10} - \frac{z_{13}}{b_{10}} \quad \text{or} \quad u_1 = \frac{(u_{10} - z_{13})}{b_{10}}, \tag{31}$$

where the parameter b_{10} is an adjustable compensating factor which decides the compensation degree.

Through the above four steps, we can finally obtain the controller as follows:

$$\begin{aligned}
e &= v_{11} - v_\psi,\\
fh &= fhan(e, v_{12}, r, h),\\
v_{11} &= v_{11} + hv_{12},\\
v_{12} &= v_{12} + h \cdot fh,\\
e_1 &= z_{11} - y_1,\\
fe &= fal(e_1, 0.5, \delta),\\
fe_1 &= fal(e_1, 0.25, \delta),\\
z_{11} &= z_{11} + h(z_{12} - \beta_{11} e_1),\\
z_{12} &= z_{12} + h(z_{13} - \beta_{12} \cdot fe + b_{10} u_1),\\
z_{13} &= z_{13} + h(-\beta_{13} \cdot fe_1),\\
s_{11} &= x_{11} - v_{11},\\
\overline{\alpha}_{11} &= v_{12} - k_{11} s_{11},\\
\tau_{11}\dot{\alpha}_{11} + \alpha_{11} &= \overline{\alpha}_{11},\\
\alpha_{11}(0) &= \overline{\alpha}_{11}(0),\\
s_{12} &= x_{12} - \alpha_{11},\\
u_{10} &= \dot{\alpha}_{11} - k_{12} s_{12},\\
u_1 &= \frac{(u_{10} - z_{13})}{b_{10}}.
\end{aligned} \tag{32}$$

4.2.2. Longitudinal Velocity Controller Design. Similar to the derivation of heading controller, the longitudinal velocity controller can be deduced based on DS-ADRC as follows:

$$\begin{aligned}
e &= v_{21} - v_u,\\
fh &= fhan(e, v_{22}, r, h),\\
v_{21} &= v_{21} + hv_2,\\
v_2 &= v_2 + h \cdot fh,\\
e_{21} &= z_{21} - y_2,\\
fe &= fal(e_1, \alpha, \delta),\\
z_{21} &= z_{21} + h(z_{22} - \beta_{21} e_1 + b_{20} u_2),\\
z_{22} &= z_{22} + h(-\beta_{22} \cdot fe),\\
s_{21} &= x_{21} - v_{21},\\
u_{20} &= v_{22} - k_{21} s_{21},\\
u_2 &= \frac{(u_{20} - z_{22})}{b_{20}}.
\end{aligned} \tag{33}$$

In (33), the definition of relevant parameters is similar to the definition in the heading controller design.

5. Simulation Results

A numerical example is given to illustrate the proposed path following control algorithm. In the simulation, our objective is to control the UUV to follow the path with speed at 1 m/s, and the sequence of points is $P = \{(5, 0), (50, 50), (50, 100), (5, 150), (5, 200), (50, 200), (50, 250)\}$. The UUV can initially rest at a random position with an unspecified attitude, supposing that it is $(x_0, y_0, \psi_0) = (0, 0, 0)$ and its velocity is $(u_0, v_0, r_0) = (0, 0, 0)$. Under the condition of constant current and other disturbances, we have a simulation comparison between the DSC and the DS-ADRC; the results are shown in Figures 4–11. Under the condition of constant current, the parameters of DSC are selected as $k_{11} = 0.8$, $\tau_{12} = 0.1$, $k_{12} = 1$, and $k_{21} = 1$, and with other disturbances the DSC parameters are $k_{11} = 0.5$, $\tau_{12} = 0.4$, $k_{12} = 1$, and $k_{21} = 2$, while for the above two conditions the parameters of the DS-ADRC both are selected as follows: $r = 0.8$, $h = 0.02$, $\delta = 0.1$, $\beta_{11} = 100$, $\beta_{12} = 300$, $\beta_{13} = 1000$, $\beta_{21} = 100$, $\beta_{22} = 1000$, $k_{11} = 1$, $k_{12} = 1$, $k_{13} = 1$, $k_{21} = 5$, $\tau_{11} = 0.1$, $b_{10} = 0.025$, and $b_{20} = 0.06$.

5.1. Path Following with Constant Current. In the north-east coordinates, we set the current velocity as 0.5 m/s and the direction as $\pi/4$. With the DSC and DS-ADRC, the relationship between UUV's "actual" path and its expected path is plotted in Figure 4. And Figures 5–7 are the UUV's cross-track error, its output of force, and moment, respectively.

Figures 4 and 5 show that the control effect of DSC and DS-ADRC is almost the same under the constant ocean current. However, from Figures 6 and 7, we can clearly see that the overshoot of DS-ADRC is smaller than the DSC and the setting time is shorter.

5.2. Path Following with Constant Current and Other Disturbances. Under the above constant current condition, we add a disturbance with which amplitude is 0.2 N·m and period is 20π, and the simulation results are as follows: Figure 8 is "actual" path and expected path under the DSC and DS-ADRC, respectively. And Figures 9–11 are the UUV's cross-track error, its output of force, and moment, respectively.

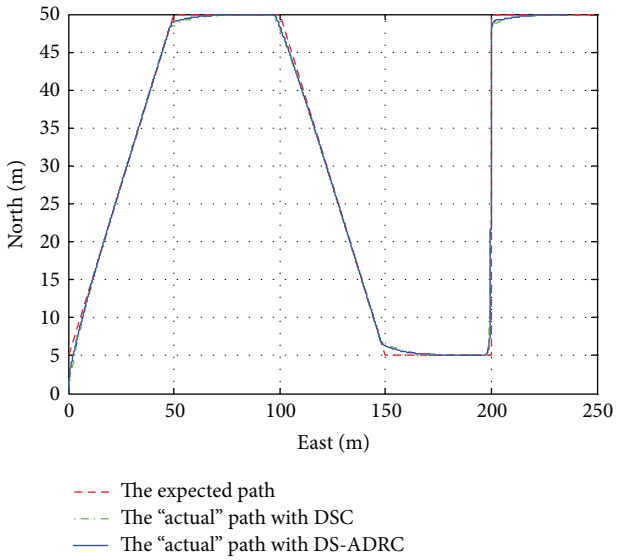

Figure 4: The responses of path following.

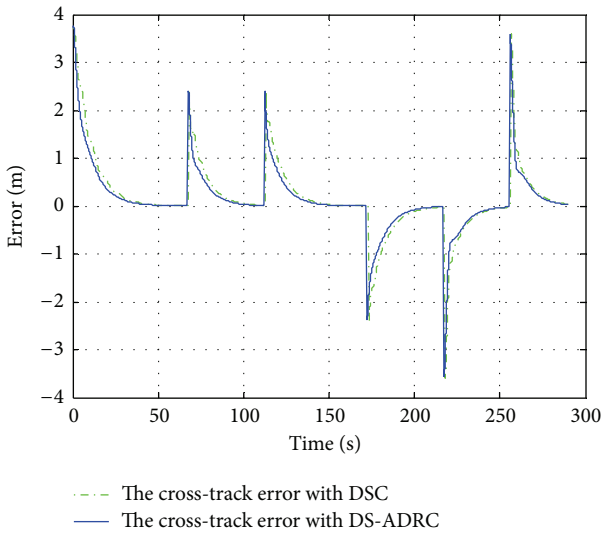

Figure 5: The cross-track error.

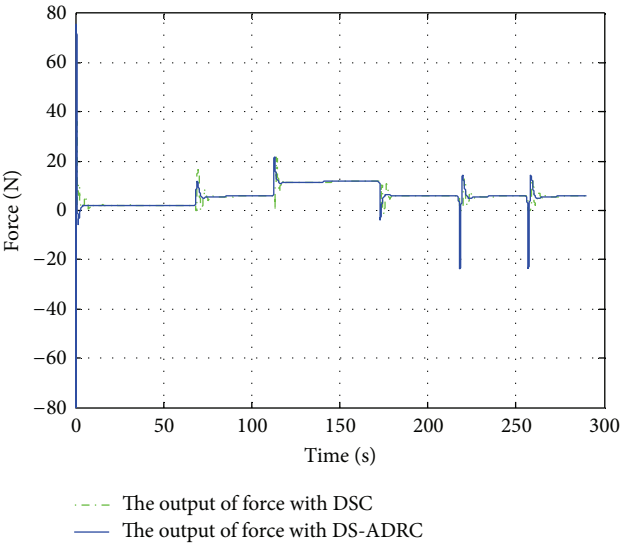

Figure 6: The output of force.

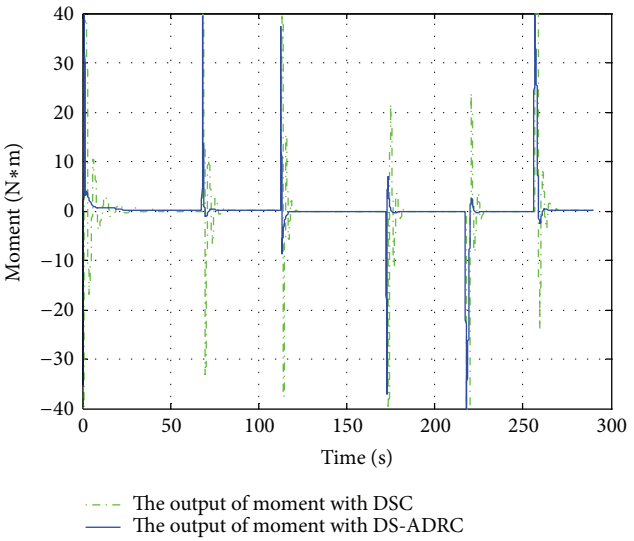

Figure 7: The output of moment.

In the presence of other disturbances, it is interesting to note that the UUV's cross-track error of the proposed method in this paper is still gradually converged to zero according to Figures 8 and 9, which show strong antidisturbances ability, while the DSC cannot. When combined with Figures 10 and 11, we can see that the overshoot of DS-ADRC is smaller and its setting time is shorter, too.

Through the above two groups of simulation contrast, it can be seen that the effects of the DSC and the DS-ADRC are similar under the constant current, but when there are other external disturbances, the effect of the DS-ADRC is much better than the simple DSC, which show strong antidisturbance characteristic to the external unknown disturbances.

6. Conclusion

This paper has presented a novel path following control method to UUV; it uses the line-of-sight guidance method to solve the real-time expectations of UUV's heading and has revised the method heading under the condition of current interference with introducing sideslip at the same time; it eliminates the stable cross-track error which is caused by the normal line-of-sight guidance method with current interference. Combining the advantages of the DSC technique and the ADRC technology, we, respectively, designed the UUV heading controller and the longitudinal velocity controller. This control method avoids the conventional dynamic surface control systems, relies on accurate mathematical models and improved antijamming capability. At the same time, the control method for a class of strict feedback forms is

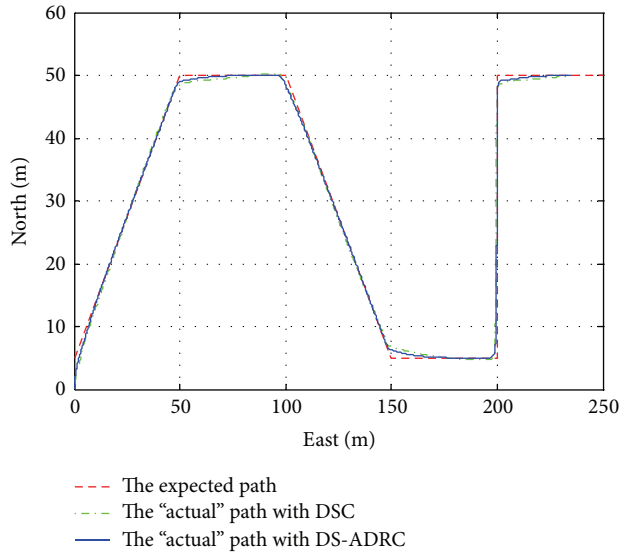

Figure 8: The responses of path following.

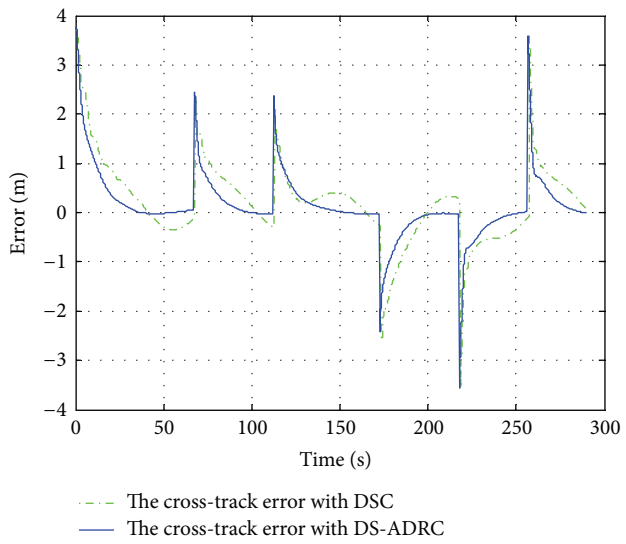

Figure 9: The cross-track error.

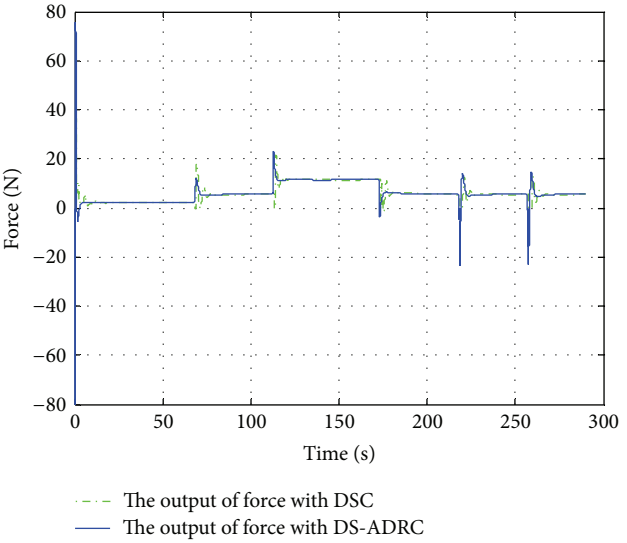

Figure 10: The output of force.

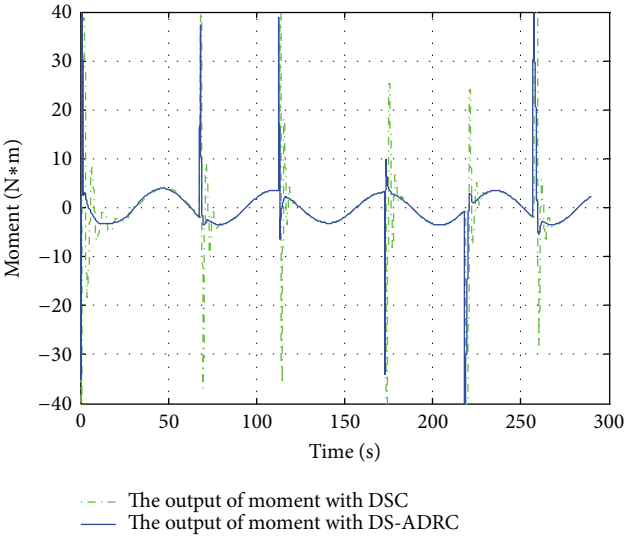

Figure 11: The output of moment.

applicable, which makes the design of the controller be in common use and be more conducive to the engineering practice. The simulation results also show that the control method has an excellent performance.

Conflict of Interests

The authors declare that there is no conflict of interests regarding the publication of this paper.

Acknowledgments

This research work is supported by the National Natural Science Foundation of China (Grant No. 51309067/E091002), the Fundamental Research Funds for the Center Universities (HEUCFX041402), and the National Defense Key Laboratory of Autonomous Underwater Vehicle Technology (9140C270208140C27004).

References

[1] R. Coulson, J. C. Lambiotte, G. Grenon, T. Pantelakis, J. Curran, and E. An, "Development of a modular docking sub-system for 12" class autonomous underwater vehicles," in *Proceedings of the Bridges across the Oceans Conference (OCEANS '04. MTTS/IEEE TECHNO-OCEAN '04)*, pp. 1745–1752, November 2004.

[2] E. Borhaug and K. Y. Fettersen, "Adaptive way-point tracking control for underactuated autonomous vehicles," in *Proceedings of the 44th IEEE Conference on Decision and Control, and the*

European Control Conference (CDC-ECC '05), pp. 4028–4034, December 2005.

[3] J. Gao, D. M. Xu, and W. S. Yan, "Global K-exponential straight-line tracking control of an underactuated AUV in three dimensions using a cascaded approach," *Control and Decision*, vol. 27, no. 9, pp. 1281–1287, 2012.

[4] P. Herman, "Modified set-point controller for underwater vehicles," *Mathematics and Computers in Simulation*, vol. 80, no. 12, pp. 2317–2328, 2010.

[5] S.-R. Oh and J. Sun, "Path following of underactuated marine surface vessels using line-of-sight based model predictive control," *Ocean Engineering*, vol. 37, no. 2-3, pp. 289–295, 2010.

[6] M. Chyba, T. Haberkorn, R. N. Smith, and S. K. Choi, "Design and implementation of time efficient trajectories for autonomous underwater vehicles," *Ocean Engineering*, vol. 35, no. 1, pp. 63–76, 2008.

[7] L. Lapierre and D. Soetanto, "Nonlinear path-following control of an AUV," *Ocean Engineering*, vol. 34, no. 11-12, pp. 1734–1744, 2007.

[8] S. Shi, W. Yan, J. Gao et al., "Path following control of an AUV in the horizontal plane with constant ocean currents," *Acta Armamentarii*, vol. 31, no. 3, pp. 375–379, 2010.

[9] D. Swaroop, J. K. Hedrick, P. P. Yip, and J. C. Gerdes, "Dynamic surface control for a class of nonlinear systems," *IEEE Transactions on Automatic Control*, vol. 45, no. 10, pp. 1893–1899, 2000.

[10] R. Li, T. Li, R. Bu, Q. Zheng, and C. L. P. Chen, "Active disturbance rejection with sliding mode control based course and path following for underactuated ships," *Mathematical Problems in Engineering*, vol. 2013, Article ID 743716, 9 pages, 2013.

[11] J. E. Refsnes, A. J. Sorensen, and K. Y. Pettersen, "Model-based output feedback control of slender-body underactuated AUVs: theory and experiments," *IEEE Transactions on Control Systems Technology*, vol. 16, no. 5, pp. 930–946, 2008.

[12] J. E. G. Refsnes, "Nonlinear model-based control of slender body AUVs," *Norwegian University of Science and Technology*, vol. 30, no. 226, pp. 229–231, 2007.

[13] T. I. Fossen, *Handbook of Marine Craft Hydrodynamics and Motion Control*, Norwegian University of Science and Technology, 2011.

[14] E. Fredriksen and K. Y. Pettersen, "Global k-exponential waypoint manoeuvering of ships," in *Proceedings of the 43rd IEEE Conference on Decision and Control*, pp. 5360–5367, 2004.

[15] J. I. A. Heming, *Study of Spatial Target Tracking Nonlinear Control of Underactuated UUV Based on Backstepping*, Harbin Engineering University, 2012.

[16] H. A. N. Jingqing, *Active Disturbance Rejection Control Technique—The Technique for Estimating and Compensating the Uncertainties*, National Defense Industry Press, 2007.